NEOPLASIA
www.neoplasia.com

Volume 15 Number 10 October 2013 pp. 1184–1195 1184

A Novel Ras Inhibitor (MDC-1016) Reduces Human Pancreatic Tumor Growth in Mice[1]

Gerardo G. Mackenzie*,†, Lauren E. Bartels*, Gang Xie*, Ioannis Papayannis*, Ninche Alston*, Kvetoslava Vrankova*, Nengtai Ouyang*,‡ and Basil Rigas*

*Division of Cancer Prevention, Department of Medicine, Stony Brook University, Stony Brook, NY; †Department of Preventive Medicine, Stony Brook University, Stony Brook, NY; ‡Medicon Pharmaceuticals, Inc, Stony Brook, NY

Abstract

Pancreatic cancer has one of the poorest prognoses among all cancers partly because of its persistent resistance to chemotherapy. The currently limited treatment options for pancreatic cancer underscore the need for more efficient agents. Because activating *Kras* mutations initiate and maintain pancreatic cancer, inhibition of this pathway should have a major therapeutic impact. We synthesized phospho-farnesylthiosalicylic acid (PFTS; MDC-1016) and evaluated its efficacy, safety, and metabolism in preclinical models of pancreatic cancer. PFTS inhibited the growth of human pancreatic cancer cells in culture in a concentration- and time-dependent manner. In an MIA PaCa-2 xenograft mouse model, PFTS at a dose of 50 and 100 mg/kg significantly reduced tumor growth by 62% and 65% ($P < .05$ *vs* vehicle control). Furthermore, PFTS prevented pancreatitis-accelerated acinar-to-ductal metaplasia in mice with activated *Kras*. PFTS appeared to be safe, with the animals showing no signs of toxicity during treatment. Following oral administration, PFTS was rapidly absorbed, metabolized to FTS and FTS glucuronide, and distributed through the blood to body organs. Mechanistically, PFTS inhibited Ras-GTP, the active form of Ras, both *in vitro* and *in vivo*, leading to the inhibition of downstream effector pathways c-RAF/mitogen-activated protein–extracellular signal–regulated kinase (ERK) kinase (MEK)/ERK1/2 kinase and phosphatidylinositol 3-kinase/AKT. In addition, PFTS proved to be a strong combination partner with phospho-valproic acid, a novel signal transducer and activator of transcription 3 (STAT3) inhibitor, displaying synergy in the inhibition of pancreatic cancer growth. In conclusion, PFTS, a direct Ras inhibitor, is an efficacious agent for the treatment of pancreatic cancer in preclinical models, deserving further evaluation.

Neoplasia (2013) 15, 1184–1195

Introduction

Pancreatic cancer, one of the most lethal malignancies in the United States, is extremely difficult to treat [1], and its prognosis remains dismal [2]. Therapeutic approaches against the advanced disease have largely failed and approximately >90% of patients diagnosed with this malignancy still die within 2 to 8 months. Surgery is rarely curative because the disease is diagnosed too late for tumor excision to be beneficial. Gemcitabine, a standard drug for pancreatic cancer therapy, is minimally effective, improving patient's survival by only months [3]. Therefore, it is critical to develop new agents for the effective management of pancreatic cancer.

Gain-of-function mutations of the *Kras* oncogene, found in about one third of human cancers, occur in >90% of pancreatic cancers [4].

Abbreviations: ERK, extracellular signal–regulated kinase; FTS, farnesylthiosalicylic acid; PFTS, phospho-farnesylthiosalicylic acid; PI3K, phosphatidylinositol 3-kinase; P-V, phospho-valproic acid

Address all correspondence to: Gerardo G. Mackenzie, PhD, Department of Preventive Medicine, Stony Brook University, HSC, T17-080, Stony Brook, NY 11794-8175. E-mail: Gerardo.Mackenzie@stonybrookmedicine.edu or Basil Rigas, MD, Division of Cancer Prevention, Stony Brook University, HSC, T17-080, Stony Brook, NY 11794-8175. E-mail: Basil.Rigas@stonybrookmedicine.edu

[1]Grant support: National Institutes of Health 5R01CA154172 (B.R.) and Department of Medicine, Stony Brook University seed grant (G.G.M.). The study sponsors had no role in the study design, in the collection, analysis, and interpretation of data, in the writing of the manuscript, nor in the decision to submit the manuscript for publication. Conflict of interest disclosure: B.R. has an equity position in Medicon Pharmaceuticals, Inc, the company that provided the test compounds; N.O. is also affiliated with the same company. All other authors declare no conflicts of interest.
Received 19 July 2013; Revised 6 September 2013; Accepted 9 September 2013

Copyright © 2013 Neoplasia Press, Inc. All rights reserved 1522-8002/13/$25.00
DOI 10.1593/neo.131368

These mutations inhibit GTP hydrolysis at the Ras-binding site, which results in excessive activity of Ras-GTP, its active form [5]. Ras-GTP stimulates four main downstream effectors, namely, Raf protein kinase, phosphatidylinositol 3-kinase (PI3K), Ral protein, and phospholipase C epsilon (PLCε). Ras regulates multiple intracellular signaling pathways, with the RAF/mitogen-activated protein–extracellular signal–regulated kinase (ERK) kinase (MEK)/ERK kinase pathway being the best understood [6,7]. In response to growth factor stimulation or oncogene activation, the RAF/MEK/ERK pathway can modulate the expression/activity of D- and E-type cyclins and cyclin-dependent kinases to regulate G_1-to-S cell cycle phase progression [8]. Not surprisingly, the RAF/MEK/ERK pathway is a major target for therapeutic intervention [9,10]. AKT, also downstream of Ras activation, regulates cell proliferation, survival/apoptosis, angiogenesis, metabolism, and protein synthesis [11,12]. AKT activation by phosphorylation, frequent in pancreatic cancer, is associated with poor prognosis [13]. Inhibition of the PI3K/AKT pathway sensitizes pancreatic cancer cells to the apoptotic effect of chemotherapy [14].

Oncogenic *Kras* is essential for both the initiation and maintenance of pancreatic cancer [15]. During all stages of pancreatic carcinogenesis, *Kras* upregulates inflammatory and signaling pathways that mediate paracrine interactions between epithelia and their surrounding microenvironment, and these Kras-dependent pathways drive tumorigenesis [16]. Given the predominant role of *Ras* oncogene in pancreatic carcinogenesis, there is an intense ongoing effort to identify inhibitors of the Ras protein [15]. *S-trans,trans*-farnesylthiosalicylic acid (FTS, Salirasib) is a Ras inhibitor [17], which interferes with Ras membrane interactions crucial for Ras-dependent transformation [18]. Goldberg et al. have shown that modifications of the FTS carboxylic group by esterification or amidation yield compounds with improved growth inhibitory activity compared to FTS [19]. We have also demonstrated that covalent modifications of several carboxylic nonsteroidal anti-inflammatory drugs generate compounds of superior efficacy and safety [20–22]. With this in mind, we synthesized the novel phospho-FTS (PFTS; MDC-1016), following the formula FTS–butane-diethyl phosphate (Figure 1*A*).

In the present study, we examined, for the first time, the efficacy, safety, and metabolism of PFTS in pancreatic cancer and its mechanism of action. Our data show that PFTS inhibits the growth of human pancreatic cancer in nude mice and prevents acinar-to-ductal metaplasia in mice with activated *Kras*. Furthermore, PFTS suppresses Ras activation, leading to strong inhibition of the RAF/MEK/ERK and PI3K/AKT pathways, and sensitizes the pancreatic cancer cells to the cytotoxic effects of phospho-valproic acid (P-V), a novel signal transducer and activator of transcription 3 (STAT3) inhibitor [23].

Materials and Methods

Reagents

PFTS (MDC-1016) and P-V (MDC-1112) were gifts from Medicon Pharmaceuticals, Inc (Stony Brook, NY). FTS was purchased from

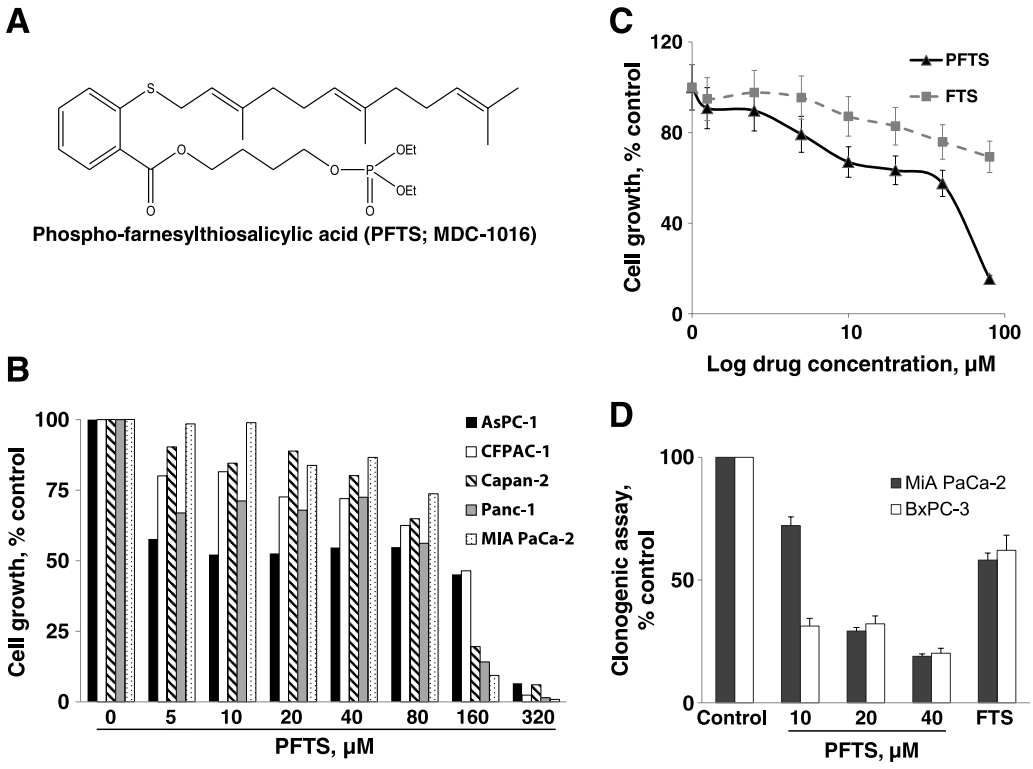

Figure 1. PFTS inhibits pancreatic cancer growth *in vitro*. (A) Chemical structure of PFTS (MDC-1016). (B) PFTS inhibits pancreatic cancer cell growth in a concentration-dependent manner. Cell growth was determined in AsPC-1, CFPAC-1, Capan-2, Panc-1, and MIA PaCa-2 after treatment with escalating concentrations of PFTS for 24 hours. Results are expressed as percentage of control. (C) PFTS inhibits MIA PaCa-2 cell growth more potently than FTS. Cell growth was determined in MIA PaCa-2 after treatment with escalating concentrations of PFTS or FTS for 72 hours. Results are expressed as percentage of control. (D) PFTS inhibits pancreatic cancer cell colony formation in a concentration-dependent manner. FTS (20 μM) led to a 42% and 38% inhibition in colony formation in MIA PaCa-2 and BxPC-3 cells.

Cayman Chemical (Ann Arbor, MI). For PFTS, FTS, and P-V, we prepared a 100 mM stock solution in DMSO. In all cell culture media, the final DMSO concentration was adjusted to 1%. Annexin V was purchased from Invitrogen (Grand Island, NY). All general solvents and reagents were of HPLC grade or the highest grade commercially available.

Cell Culture

Human pancreatic cancer (BxPC-3, AsPC-1, CFPAC-1, Capan-2, Panc-1, and MIA PaCa-2) cell lines were grown as monolayers in the specific medium suggested by the American Type Culture Collection (Manassas, VA) and supplemented with 10% fetal calf serum (Mediatech, Herndon, VA), penicillin (50 U/ml), and streptomycin (50 μg/ml; Life Technologies, Grand Island, NY). Cells were incubated at 37°C in 5% CO_2. Cells were seeded at 5.5×10^4 cells/cm^2 and allowed to attach overnight, and the following morning, the cells were treated with the test agents as indicated.

Cell Viability Assay

Following the treatment with various concentrations of PFTS or FTS for 24, 48, or 72 hours, the reduction of 3-(4,5-dimethylthiazol-2-yl)-2,5-diphenyltetrazolium bromide dye was determined according to the manufacturer's protocol (Promega, Madison, WI).

Colony Assay

MIA PaCa-2 and BxPC-3 cells, plated onto six-well plates (3000 cells per well), were treated with PFTS or FTS for 10 days, with their media replaced every 3 days. The cells were then stained with 1% crystal violet in borate-buffered saline (0.1 M, pH 9.3) and 0.02% ethanol. Following lysis with 1% sodium dodecyl sulfate (SDS), the absorbance was read at 570 nm.

Apoptosis

To measure apoptosis and necrosis, cells (1.0×10^5 cells per well) were treated with various concentrations of PFTS or P-V or both for 24 hours. Briefly, after the treatment with the test compounds, cells were trypsinized and stained with annexin V–fluorescein isothiocyanate (×100 dilution; Invitrogen) and propidium iodide (0.5 μg/ml; Sigma, St Louis, MO), and the fluorescence intensities were analyzed by FACSCalibur (BD Biosciences, San Jose, CA).

Western Blot Analysis

Total cell fractions were obtained as previously described [24]. Aliquots of total fractions containing 25 to 40 μg of protein were separated by reducing 10% to 12.5% (wt/vol) polyacrylamide gel electrophoresis (PAGE) and electroblotted to nitrocellulose membranes. The membranes were probed overnight with Ras (Thermo Scientific, Rockford, IL), c-RAF (Cat. No. 9422), p-c-RAF Ser^{259} (Cat. No. 9422), p-ERK1/2 Thr^{202}/Tyr^{204} (Cat. No. 4376), ERK1/2 (Cat. No. 4370), p-MEK1/2 $Ser^{217}/^{221}$ (Cat. No. 9154), MEK1/2 (Cat. No. 9122), p-AKT Ser^{473} (Cat. No. 4060), and AKT (Cat. No. 4691; Cell Signaling Technology, Danvers, MA) antibodies (1:1000 dilution). β-Actin (Sigma) was used as the loading control. After incubation, for 90 minutes at room temperature, in the presence of the secondary antibody (HRP conjugated; 1:5000 dilution), the conjugates were visualized by chemiluminescence.

Ras Pull-Down Assays and Immunoblot Analysis

Freshly isolated tumors were weighed and then homogenized (10% wt/vol) in lysis buffer [25]. Total amounts of Ras were determined in samples (60 μg of protein) of each lysate by SDS-PAGE followed by immunoblot analysis with pan-Ras antibody (Thermo Scientific). The amounts of Ras-GTP in 800 μg of protein of total tumor lysates were determined by the glutathione *S*-transferase–Ras-binding domain of Raf pull-down assay, as described elsewhere [25]. The pull-down Ras-GTP was subjected to SDS-PAGE followed by immunoblot analysis with pan-Ras Ab. Protein bands were visualized by enhanced chemiluminescence and quantified by densitometry using ImageJ computer software (National Institutes of Health, Bethesda, MD).

Animal Studies

All animal studies were approved by the Institutional Animal Care and Use Committee at Stony Brook University (Stony Brook, NY).

Toxicity of PFTS in mice. We evaluated in mice the potential acute toxicity of PFTS. Groups of 6-week-old female BALB/c mice (five mice per group) were given 0, 75, 150, 250, and 350 mg/kg PFTS by oral gavage once a day for 3 weeks. Body weights were recorded twice weekly. Animals were killed at 3 weeks, and their organs were examined for any signs of toxicity.

Pharmacokinetic studies in mice. PFTS (200 mg/kg) or an equimolar dose of FTS (126 mg/kg) was administered as a single treatment by gastric gavage to female BALB/c mice. Mice were killed at various time points after drug administration, and blood and organs were collected. Blood was immediately centrifuged, and the resulting plasma was deproteinized by immediately mixing it with a two-fold volume of CH_3CN. PFTS, FTS, and its metabolites were analyzed by HPLC as described below.

Efficacy study in nude mouse xenografts. Female immune-deficient BALB/c nude mice at 6 weeks of age were purchased from Charles River Laboratories (Wilmington, MA) and were maintained in pathogen-free conditions with irradiated chow. Animals were bilaterally, subcutaneously (s.c.) injected with 1.5×10^6 MIA PaCa-2 cells per tumor in 0.1 ml of sterile phosphate-buffered saline. When MIA PaCa-2 cells reached palpable tumors, mice ($n = 7$ per group) were divided randomly into three groups receiving control, 50 mg/kg PFTS, or 100 mg/kg PFTS in corn oil, which were given orally to mice five times per week during 25 days. Only corn oil was given to the untreated control mice. Body weight was measured once a week, whereas tumors were measured twice weekly. Tumor sizes were calculated by the following formula: [length × width × (length + width/2) × 0.56] in millimeters. At the end of the experiments, animals were killed by CO_2 asphyxiation and tumor weights were measured after their careful resection. Tumor tissue was collected for analysis.

p48-Cre;LSL-$Kras^{G12D}$ mouse studies. *p48-Cre;LSL-$Kras^{G12D}$* mice (2-3 months old) in C57Bl/6J background were injected intraperitoneally with cerulein (50 μg/kg hourly, four times per day, 2 days per week; 3 days of injection). Cerulein-injected mice were divided into vehicle ($n = 3$) and PFTS ($n = 3$) groups. PFTS (100 mg/kg) was given 5 days per week by oral gavage, starting the treatment on

the day of the first cerulein injection. On day 9, mice were killed and the pancreas was excised, fixed in formalin, and processed for morphologic and immunohistochemical studies.

Immunohistochemistry

Immunohistochemical staining for Ki-67, α-amylase, p-c-RAF, and p-ERK1/2 was performed as previously described [26].

Determination of Apoptosis

Apoptosis was determined immunohistochemically by the terminal deoxynucleotidyl transferase–mediated deoxyuridine triphosphate–biotin nick end labeling (TUNEL) assay [22]. Formalin-fixed tissues were determined using the *In Situ* Cell Death Detection Kit, POD (Roche, Indianapolis, IN) as per the manufacturer's instructions. Treatment of samples with DNAse I was used as positive control.

Scoring for TUNEL and immunohistochemistry. At least 10 fields per sample were scored by an investigator blinded to the identity of the samples. We calculated the percentage of proliferating and apoptotic cells by dividing the number of labeled cells by the number of cells in each field and multiplying by 100.

HPLC-UV Analysis

The HPLC system consisted of a Waters Alliance 2695 Separation Module equipped with a Waters 2998 Photodiode Array Detector (262 nm) and a Thermo Hypersil BDS C18 column (150 × 4.6 mm, particle size of 3 μm). The mobile phase consisted of a gradient between an aqueous phase [trifluoroacetic acid/CH_3CN/H_2O, 0.1:4.9:95 (vol/vol/vol)] and CH_3CN at a flow rate of 1 ml/min at 30°C. A gradient elution from 50% to 100% CH_3CN from 0 to 6 minutes was applied and maintained at 100% CH_3CN until 8 minutes.

Liquid Chromatography-Tandem Mass Spectrometry Analysis

The LC-MS/MS system consisted of Thermo TSQ Quantum Access (Thermo Fisher Scientific, Waltham, MA) triple quadrupole mass spectrometer interfaced by an electrospray ionization probe with an UltiMate 3000 HPLC system (Dionex Corporation, Sunnyvale, CA). Chromatographic separations were achieved on a Luna C18 column (150 × 2 mm), and the mobile phase consisted of a gradient from 10% to 95% CH_3CN.

Statistical Analysis

The data, obtained from at least three independent experiments, were expressed as means ± SEM. Statistical evaluation was performed by one-factor analysis of variance followed by Tukey test for multiple comparisons. $P < .05$ was regarded statistically significant.

Results

PFTS Inhibits the Growth of Human Pancreatic Cancer Cells in Culture

Our first goal was to establish the efficacy of PFTS in pancreatic cancer cells in culture. We treated a panel of five human pancreatic cancer cell lines with or without escalating concentrations of PFTS (5-320 μM) for 24 hours. As shown in Figure 1*B*, PFTS reduces pancreatic cancer cell growth in a concentration-dependent manner in all the cell lines tested. For instance, at 24 hours, PFTS (5 μM) reduced cell growth in AsPC-1 and Panc-1 cells by 43% and 34% ($P < .05$), respectively.

We then compared the potency of PFTS to that of FTS, its parent compound, in MIA PaCa-2–treated cells for 72 hours. PFTS inhibited the growth of MIA PaCa-2 pancreatic cancer cells more potently than FTS (Figure 1*C*); their respective 72-hour half maximal inhibitory concentration (IC_{50}) values were 44.1 ± 2.8 μM (mean ± SEM for this and all subsequent values) and >80 μM, representing a >1.8-fold enhancement.

We also examined the effect of PFTS and FTS on colony formation in two pancreatic cancer cell lines. PFTS inhibited colony formation in a concentration-dependent manner and was significantly superior to FTS (Figure 1*D*). For example, PFTS (20 μM) reduced colony formation by 71% and 68%, whereas FTS, at the same concentration, reduced it by 42% and 38% in MIA PaCa-2 and BxPC-3 cells, respectively. The difference in potency between PFTS and FTS groups was significant ($P < .01$) in both cell lines.

PFTS Inhibits the Growth of Human Pancreatic Xenografts in Nude Mice

We next assessed the *in vivo* chemotherapeutic potential of PFTS using a pancreatic cancer xenograft model. MIA PaCa-2 cells s.c. injected into athymic nude mice gave rise to exponentially growing tumors. Once the tumors reached ~200 mm^3, the mice were treated orally either with PFTS (50 or 100 mg/kg) or with vehicle. On day 25 of treatment, the percentage of tumor volume increase over baseline for the vehicle control, PFTS (50 mg/kg per day), and PFTS (100 mg/kg per day) groups were 294.2 ± 68.4, 172 ± 60.6, and 167 ± 50.3, respectively. Although PFTS treatment did not lead to tumor regression, 50 and 100 mg/kg PFTS presented a 62% and 65% reduction in the rate of tumor growth from baseline for the two PFTS doses, respectively ($P < .05$ for both; Figure 2, *A* and *B*).

To investigate the mechanism by which PFTS reduced tumor growth, we determined cell proliferation (Ki-67 immunohistochemistry) and apoptosis (TUNEL assay) in tumor tissue sections from control and PFTS-treated mice. Both Ki-67 immunohistochemistry (IHC) and TUNEL staining showed nuclear positive. The percentage of positive cells in the tumors for both Ki-67 and TUNEL staining was counted and calculated as the results. Compared to controls, PFTS (100 mg/kg) inhibited cell proliferation by 44% ($P < .05$) and increased apoptosis by 102% ($P < .01$; Figure 2*C*).

PFTS Prevents against Pancreatitis-Accelerated Pancreatic Intraepithelial Neoplasia Formation in Mice with Activated Kras

Because chronic pancreatitis is a significant risk factor for pancreatic cancer [27,28], we investigated whether PFTS inhibits Kras-driven pancreatic carcinogenesis in the setting of pancreatitis induced by cerulein.

In *p48-Cre;Kras^{G12D}* mice, cerulein treatment (4 hourly injections, two times per week) induced acinar-to-ductal metaplasia in all vehicle-treated animals, significantly replacing the exocrine compartment (Figure 3). This effect was accompanied by lower expression of amylase, an acinar marker, and enhanced Alcian blue staining, which

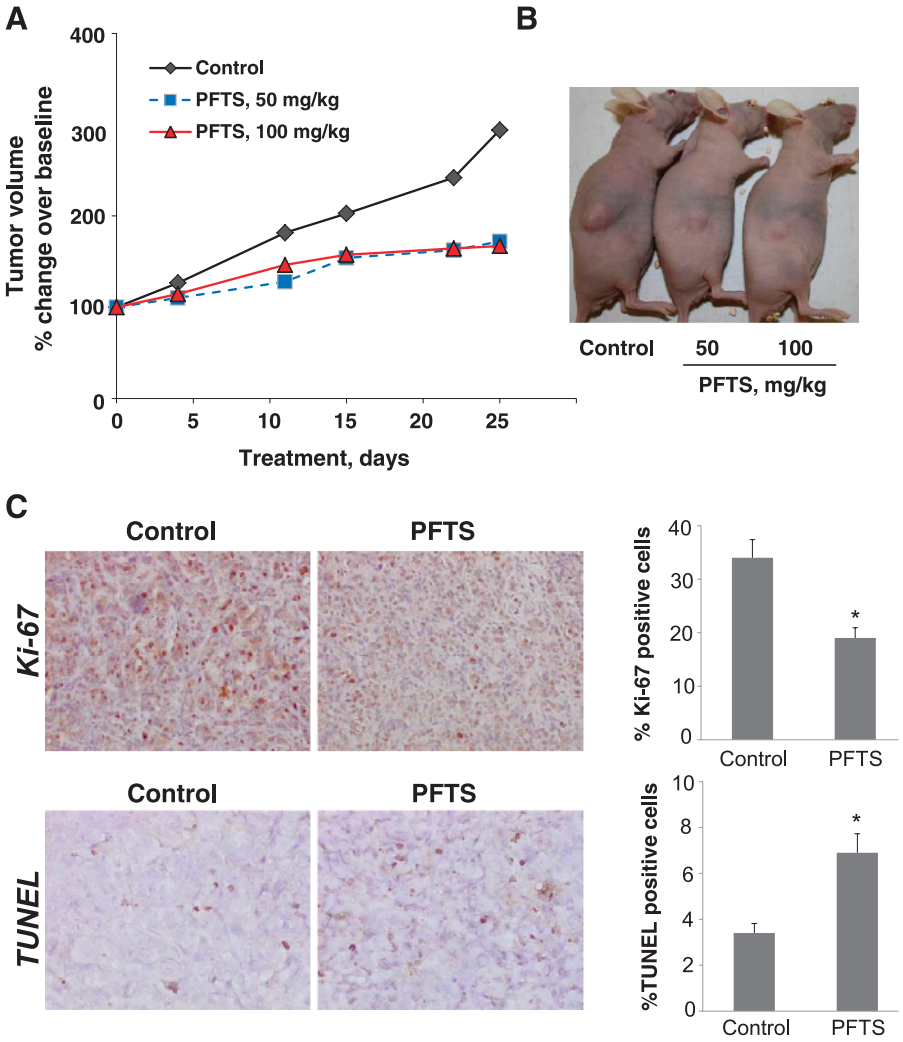

Figure 2. PFTS inhibits the growth of pancreatic cancer xenografts. (A) Inhibition of MIA PaCa-2 tumor growth in nude mouse by PFTS. MIA PaCa-2 cells were injected s.c. into the flank areas of nude mice, and when palpable tumors were observed, the mice received PFTS (50 or 100 mg/kg per day) in corn oil or just corn oil (control) by oral gavage for 25 days. (B) Representative image of mice bearing tumors. (C) Representative images (×20) of tissue sections from xenograft tumors treated with either vehicle (control) or PFTS and stained for Ki-67 expression (proliferation marker) or by the TUNEL method (apoptosis). The proliferation and apoptosis indices of xenograft tumors were determined and expressed as means ± SEM (*P < .05 for both).

characterizes pancreatic intraepithelial neoplasias (PanINs) [29]. PFTS (100 mg/kg) treatment prevented cerulein-induced acinar-to-ductal metaplasia, reducing PanIN formation, an effect associated with four-fold increased amylase expression (P < .05) and 43% decreased Alcian blue staining areas compared to cerulein-treated controls (P < .05; Figure 3).

Safety of PFTS in Mice

In the efficacy study mentioned above, PFTS was well tolerated, with the mice showing no weight loss or other signs of toxicity during treatment. For instance, on the day before killing, body weight in the three groups of mice was given as follows: control = 21.1 ± 1.5 g; PFTS (50 mg/kg) = 20.7 ± 0.7 g; PFTS (100 mg/kg) = 21.4 ± 1.5 g.

We also examined the toxicity of PFTS in mice. Groups of 6-week-old female BALB/c mice (five mice per group) were given 0, 75, 150, 250, and 350 mg/kg PFTS by oral gavage once a day for 3 weeks. Body weights were recorded twice weekly. All of the PFTS-treated animals showed no signs of toxicity and were alive and healthy throughout the study. The body weights of vehicle- and PFTS-treated animals were comparable throughout the study.

Finally, we determined that the (subchronic) maximum tolerated dose of PFTS (3-week period of observation) is at least 350 mg/kg per day.

Pharmacokinetic Study of PFTS

To study the pharmacokinetic properties of PFTS, we administered to mice by oral gavage a single dose of PFTS (200 mg/kg) or an equimolar dose of FTS (126 mg/kg). Two major metabolites, FTS and FTS glucuronide, were readily detected in the plasma. FTS glucuronide was identified by LC-MS/MS analysis. The mass spectrum of FTS glucuronide showed an $[M\text{-}H]^-$ ion at m/z 533, which was further fragmented at its glucuronide bond to generate m/z 357 (Figure 4*A*).

Following PFTS administration, the plasma levels of the two metabolites increased rapidly and their concentration peaked 1 hour

later. Specifically for FTS, T_{max} = 1 hour and C_{max} = 29.7 μM, and for FTS glucuronide, T_{max} = 1 hour and C_{max} = 10.3 μM (Figure 4*B*), indicating that PFTS was rapidly absorbed, metabolized, and distributed to the blood. The level of intact PFTS in murine plasma was ~1 μM.

With FTS, we obtained similar results: for FTS, T_{max} = 1 hour and C_{max} = 19.8 μM, and for FTS glucuronide, T_{max} = 2 hours and C_{max} = 37.4 μM (Figure 4*B*). When we calculated the $AUC_{0–24\ hours}$ for these compounds, it became clear that both generated similar cumulative levels of FTS [area under the curve $(AUC)_{0–24\ hours}$ for PFTS was 114 μMxh and 116 μMxh for FTS]. In contrast, the glucuronidation of PFTS is less extensive than that of FTS. For example, the corresponding $AUC_{0–24\ hours}$ values for FTS glucuronide were 50.9 and 187.8 μMxh, indicating that PFTS generated 3.7-fold less of this metabolite compared to an equimolar amount of FTS (Figure 4*B*).

To evaluate the biodistribution of PFTS in mice, we measured the levels of PFTS and its metabolites in the heart, kidney, liver, pancreas, and intestine. One hour following its administration by oral gavage, PFTS was detected in large amounts in the intestine and, to a lesser extent, in the pancreas. In the liver, kidney, and heart, only FTS and FTS glucuronide were detectable (Figure 4*C*). Thus, despite its rapid hydrolysis in blood, PFTS can partially survive in appreciable amounts in the pancreas but is rapidly metabolized by the liver.

One hour following FTS administration, FTS and FTS glucuronide were detected in all the organs tested. Interestingly, the levels of FTS glucuronide were significantly higher in the intestine, kidney, and liver compared to the heart and pancreas (Figure 4*C*), and these were almost double than those obtained with PFTS. Taken together with the plasma levels, these findings make it clear that glucuronidation is a

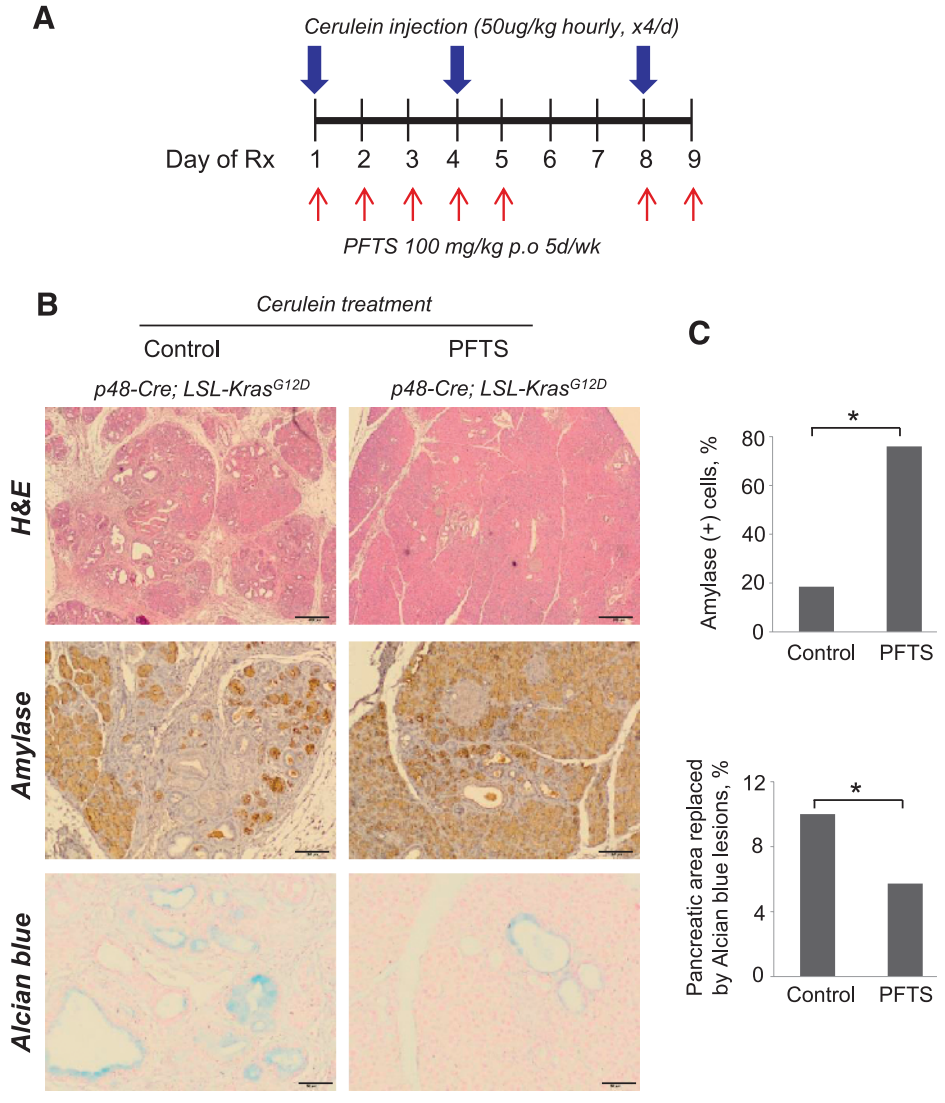

Figure 3. PFTS protects against acute pancreatitis-accelerated PanIN formation. (A) Cerulein treatment protocol. Mice with activated Kras (*p48-Cre;LSL-Kras*^{G12D}) were injected with cerulein and killed 9 days post-injection. At the day of the first injection of cerulein, mice were treated with PFTS (100 mg/kg per day) as shown. (B) The following stains were performed. (Top) hematoxylin and eosin (H&E) stain. Fewer ductal and more acinar structures were observed in the PFTS-treated mice (×4); scale bars, 200 μm. (Middle) Amylase. PFTS-treated mice retained larger areas of amylase-expressing epithelium (×10); scale bars, 100 μm. (Bottom) Alcian blue stain (×20); scale bars, 50 μm. (C) The percentages of amylase-positive area and Alcian blue–positive staining per field were quantified and expressed as means ± SEM (*$P < .05$ for both).

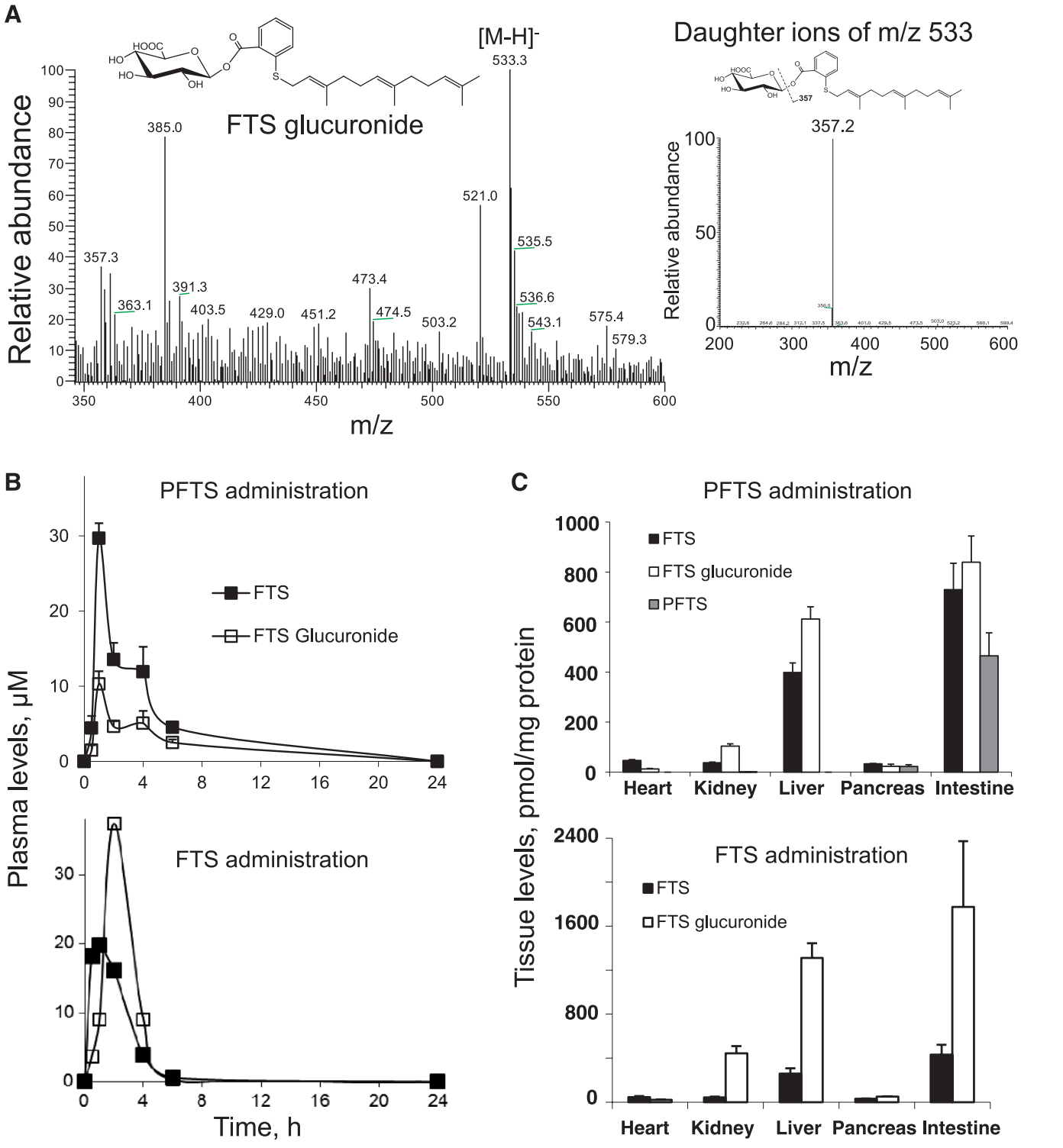

Figure 4. Pharmacokinetic analysis of PFTS. (A) MS spectrum of a major metabolite of PFTS. (Left) MS spectrum of the FTS glucuronide fraction collected from HPLC. (Right) MS/MS spectrum of the major fragment ions of the FTS glucuronide ion. (B) The pharmacokinetics of PFTS and FTS administered in corn oil to mice. PFTS (200 mg/kg) or an equimolar dose of FTS (126 mg/kg) was administered to mice as a single dose orally in corn oil. Plasma levels of PFTS and FTS metabolites were determined at the times shown. (C) Biodistribution of PFTS and FTS in mouse tissues after 1 hour of its administration. The heart, kidneys, liver, pancreas, and intestines of the mice studied in B were harvested, and PFTS, FTS, and its metabolites were measured as in Materials and Methods section. Data were expressed as picomoles of the metabolite per milligram of protein in each tissue.

significant pathway for both PFTS and FTS, but quantitatively, it is far more important for the latter.

PFTS Inhibits Ras Activation and Its Downstream Effectors ERK and AKT

We examined whether the pancreatic cancer growth inhibitory effect of PFTS was associated with down-regulation of Ras signaling, as is the case with FTS [19,25]. For this purpose, we used the Ras-GTP pull-down assay. In Panc-1 cells, PFTS significantly inhibited active Ras (Ras-GTP) in a concentration-dependent manner, and this decrease was more pronounced than the one observed with FTS (Figure 5). The inhibition of Ras by PFTS led to a significant time-dependent inhibition of the RAF/MEK/ERK and PI3K/AKT pathways, two downstream effectors of Ras (Figure 5*C*).

The inhibition of Ras by PFTS was confirmed *in vivo*. We used the Ras-GTP pull-down assay to test the capacity of PFTS to inhibit active Ras in fresh protein lysates from MIA PaCa-2 xenografts. Compared to controls, 50 and 100 mg/kg PFTS reduced RAS activation in xenografts by 62% and 70%, respectively ($P < .01$ for both; Figure 6*A*). The suppression of Ras was accompanied by inhibition of p-ERK and p-AKT, as determined by immunoblot analysis (Figure 6*B*). Moreover, immunostaining of xenograft tissue sections revealed that PFTS reduced the expression of p-c-RAF and p-ERK1/2 by 73% and 71%, respectively, compared to control ($P < .01$; Figure 6*C*).

Taken together, these *in vivo* results, in agreement with our *in vitro* results, suggest that Ras is a critical molecular target of PFTS, likely accounting for its pancreatic cancer growth inhibitory effect.

PFTS Synergizes with P-V to Enhance Human Pancreatic Cancer Growth Inhibition

Growing preclinical and clinical evidence indicates that combination therapies increase the anticancer efficacy without increasing toxicity [30]. Besides Ras signaling, STAT3, which is overexpressed in pancreatic cancer, has been described as a key driver of the progression into advanced pancreatic cancer [29,31]. Therefore, we evaluated in BxPC-3 and MIA PaCa-2 cells the potential synergy between PFTS and P-V, a novel STAT3 inhibitor, efficacious in pancreatic cancer [23]. Using isobolograms, we observed that in MIA PaCa-2 cells, there is a clear-cut pharmacological synergy between PFTS

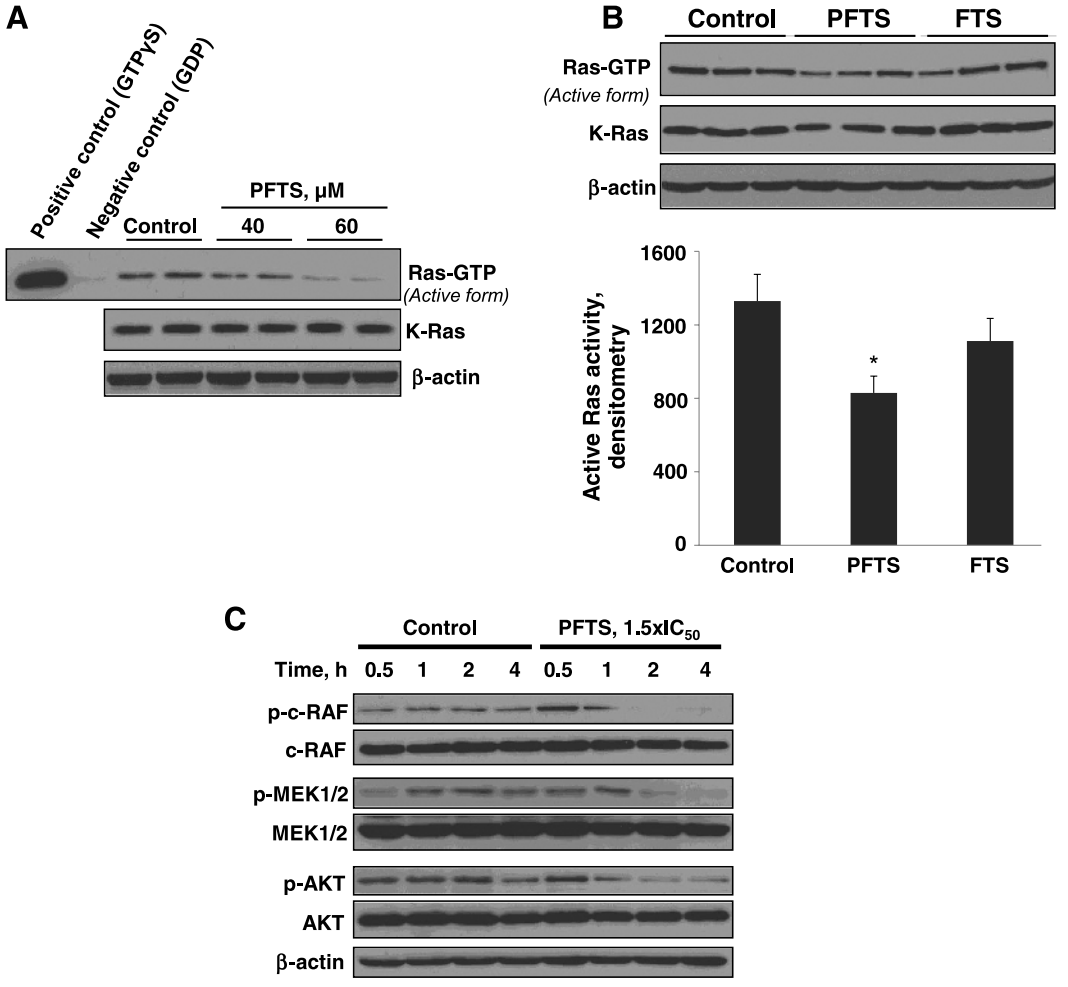

Figure 5. PFTS inhibits Ras activation and reduces ERK1/2 and AKT activation in pancreatic cancer cells. (A) Immunoblots of Ras-GTP (active Ras) and total Kras in Panc-1 cells treated without or with PFTS, as indicated, for 24 hours. (B) Immunoblots of Ras-GTP (active Ras) in cell protein extracts from Panc-1 cells treated with 50 μM PFTS or 50 μM FTS for 24 hours. *$P < .05$ *versus* control. (C) Immunoblots of p-c-RAF, c-RAF, p-MEK, MEK, p-AKT, and AKT in whole-cell protein extracts from Panc-1 cells treated with PFTS as indicated. Loading control, β-actin.

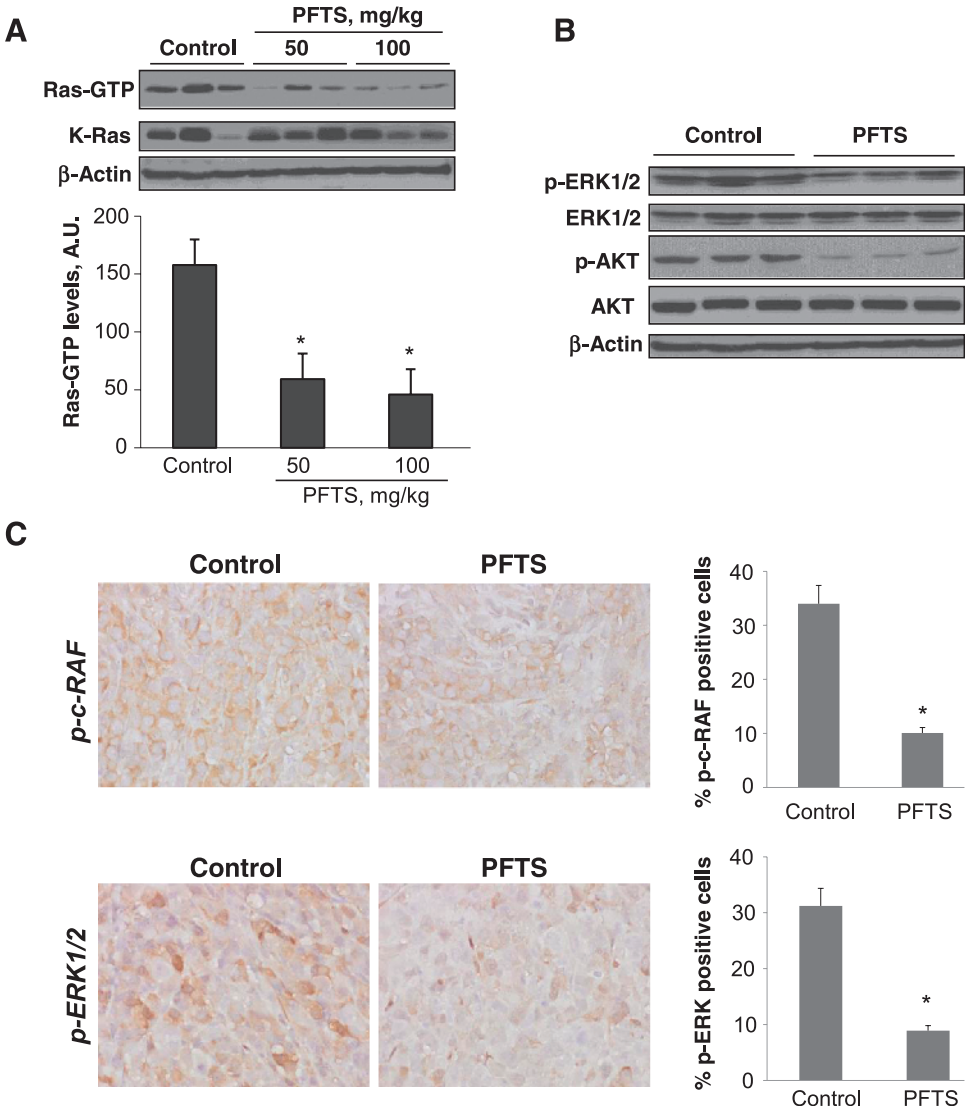

Figure 6. PFTS inhibits Ras activation and reduces ERK1/2 and AKT activation in pancreatic xenografts. (A) Immunoblots of Ras-GTP (active Ras) and total Kras. Samples of three control tumors and of three tumors of each PFTS-treated mouse were subjected to the determination of total Kras and Ras-GTP. (Upper panel) Immunoblots. (Lower panel) Levels of Ras-GTP were quantified by densitometry (AU) and expressed as mean ± SD values. *$P < .01$ *versus* control. (B) Immunoblots of p-ERK, ERK, p-AKT, and AKT in whole-cell protein extracts from MIA PaCa-2 xenografts. Loading control, β-actin. (C) Images of tissue sections from xenograft tumors treated without or with PFTS and stained for p-ERK expression. The percentage of p-ERK–positive cells per field was determined and expressed as mean ± SEM (*$P < .03$).

and P-V in inhibiting cell growth (Figure 7, *A* and *B*). However, in BxPC-3 cells, the cytotoxic effect of PFTS and P-V was only additive. In addition, as shown in Figure 7*C*, there is also a clear-cut synergistic effect in the induction of apoptosis in MIA PaCa-2 cells but not in BxPC-3 cells. After 24 hours of treatment, PFTS (1× IC_{50}) plus P-V (1× IC_{50}) increased annexin V(+) cells by 4.5-fold over control compared to 2.4-fold for P-V alone and 1.9-fold for PFTS (Figure 7*C*). These results suggest that P-V could be a useful combination partner of PFTS in the treatment of Ras mutant cancers.

Discussion

Inoperable pancreatic cancer remains a devastating malignancy because of the lack of efficacious treatments. In the present study, we show that the novel PFTS is effective and safe against pancreatic cancer in mice by inhibiting Ras activation and its downstream effectors ERK1/2 and AKT pathways. The anticancer efficacy of PFTS, accompanied by its apparent lack of toxicity, makes it a promising drug candidate for the treatment of pancreatic cancer.

Gain-of-function mutations in the *Kras* oncogene constitute one of the main genetic alterations found in pancreatic cancer. Kras activity is not only essential for pancreatic tumor formation and development, but also, at least in mice, the requirement for Kras is continuous [15,16]. Further stressing the importance of Kras is the finding that inactivation of oncogenic Ras in mice results in tumor shrinkage [16]. Thus, Ras is widely considered a therapeutic target of exceptional importance.

The novel PFTS is a strong inhibitor of Ras activation. Both PFTS and FTS produced a robust inhibition of RAS activation without a significant decrease in total Ras levels. This is in contrast to findings by other groups who have demonstrated that the inhibition of Ras activation is followed by a decrease in the levels of total Ras [17,19]. At present, there is no readily available explanation for this seeming discrepancy.

PFTS was generated by modifying the carboxylic group of FTS to enhance its efficacy, as we have done with other anticancer agents [20–22,26,32,33]. PFTS has a higher capacity to inhibit Ras activity and is more effective than FTS in suppressing pancreatic cancer cell growth. That PFTS is more effective than FTS could be attributed directly to the butane-diethyl phosphate modification that was added to be parent moiety. Of note, we have also demonstrated that similar modifications of several carboxylic nonsteroidal anti-inflammatory drugs generated compounds of superior efficacy and safety [20–22]. In agreement to our results, Goldberg et al. demonstrated that specific modifications of the carboxylic group of FTS by esterification or amidation yield compounds with improved growth inhibitory activity compared to FTS [19].

We used two complementary preclinical models to evaluate the anticancer effect of PFTS in pancreatic cancer. These included 1) an MIA PaCa-2 *Kras* mutant xenograft model in nude mice and 2) a *Kras*-driven pancreatic carcinogenesis mouse model. On the basis of

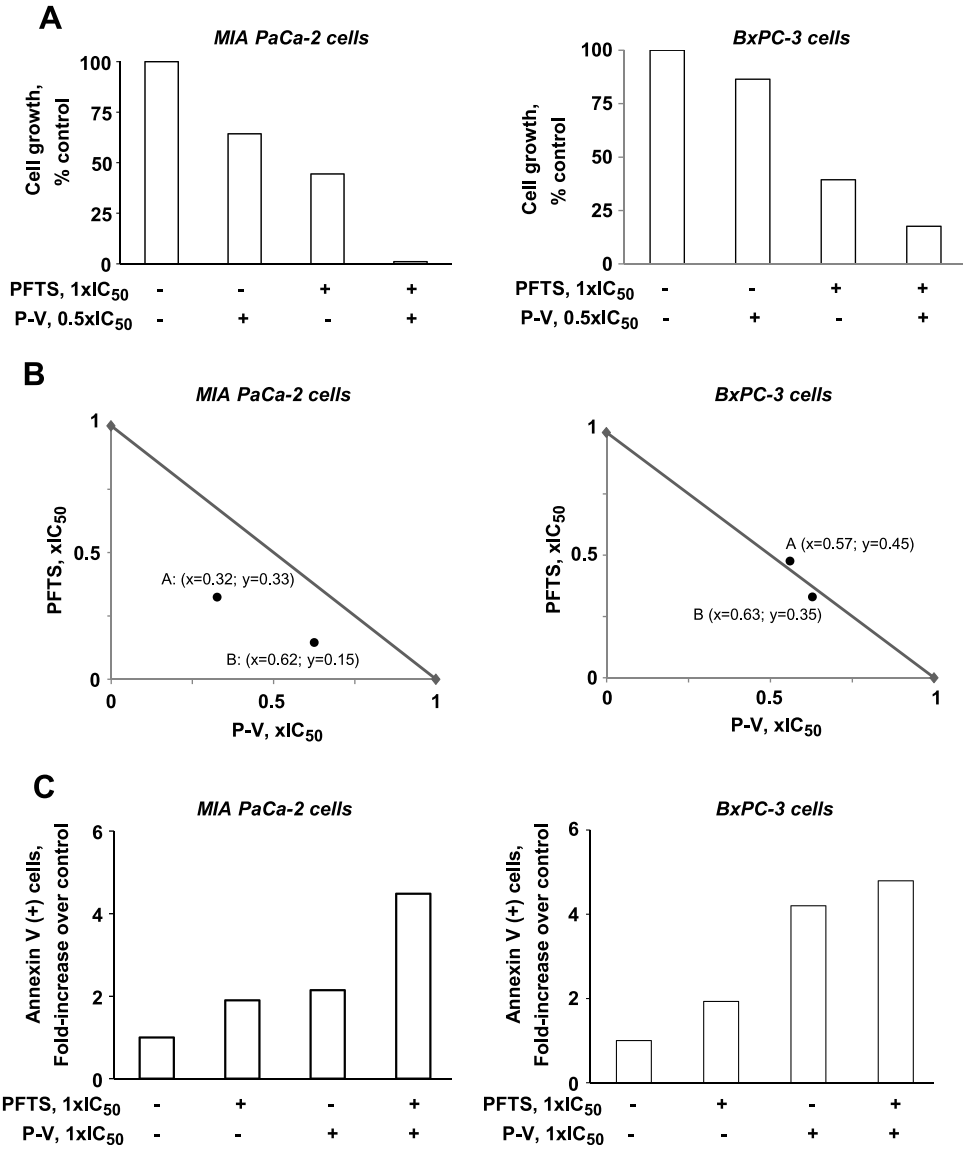

Figure 7. P-V enhances PFTS-induced inhibition of pancreatic cancer cell growth. (A) Cell viability was determined in MIA PaCa-2 and BxPC-3 cells after 24 hours of incubation with P-V, PFTS, or both. Results are expressed as percentage of control. (B) In the isobolograms, the additivity line connects the IC_{50} value of each compound used alone. A and B represent two different dose pairs of each compound (their respective concentrations are shown in parentheses). The location of both A and B below the additivity line signifies synergy, whereas the location of the points close to the line signifies additivity. (C) The percentages of apoptotic cells were determined by flow cytometry using dual staining (annexin V and propidium iodide). The percentage of annexin V(+) cells was calculated, and results are expressed as percentage of control. Of note, the drug concentrations refer to the 24-hour IC_{50} for each drug in each particular cell line, as calculated by the 3-(4,5-dimethylthiazol-2-yl)-2,5-diphenyltetrazolium bromide assay.

our findings from human pancreatic cancer xenografts, which allowed us to evaluate the therapeutic potential of PFTS, the inhibition of pancreatic cancer growth by PFTS was strong, significantly reducing the rate of growth of MIA PaCa-2 tumors by up to 65% in nude mice without causing any toxic side effects. We further examined the chemopreventive effect of PFTS on the earliest phases of pancreatic cancer development using a Kras/pancreatitis-associated carcinogenesis model. In this model, *Kras* mutations are important contributors to the altered pancreatic plasticity and acinar-to-ductal metaplasia [16]. PFTS was efficacious in reducing acinar-to-ductal metaplasia and in preventing PanIN formation. Overall, these two preclinical models indicate that PFTS is efficacious in pancreatic cancer.

Our animal studies assessed multiple parameters of toxicity. PFTS was well tolerated, showing essentially no signs of toxicity. This finding is in agreement with previous reports showing that selective blocking of activated Ras proteins inhibits Ras transformation in animal models, with no accompanying toxicity [25]. The pharmacokinetic and biodistribution studies demonstrated that following its administration to mice, PFTS is rapidly absorbed, metabolized, and distributed into blood and other tissues. In addition to intact PFTS, we have identified two additional metabolites, FTS and FTS glucuronide, which are present at substantial concentrations. A striking finding was the substantially (3.7-fold less) limited glucuronidation of PFTS compared to FTS, despite the fact that both compounds generated essentially identical plasma levels of FTS. It is conceivable that PFTS may activate additional metabolic pathways that we have not identified or it suppresses directly the glucuronidation pathway.

By targeting Ras, PFTS inhibited two prominent downstream pathways, RAF/MEK/ERK and PI3K/AKT. The Ras-activated RAF/MEK/ERK pathway has been implicated in a wide variety of processes in the cancer cell including the regulation of cell mortality, apoptosis, angiogenesis, invasion and metastasis, and cell division cycle [8]. A consequence of the suppression of Ras activation by PFTS is the inhibition of ERK phosphorylation both *in vitro* and *in vivo*. Because of the requirement of RAF/MEK/ERK signaling in the aberrant behavior of the pancreatic cancer cell, its downregulation could explain, in part, the reduction in cell proliferation observed in PFTS-treated tumors.

The activation of AKT is common in pancreatic cancer, and its inhibition sensitizes cells to the apoptotic effects of chemotherapy [13,14]. Activation of AKT by upstream signals, such as Ras, confers a survival advantage that includes resistance to the apoptotic effects of chemotherapy and radiotherapy. Remarkably, there is a significant correlation between activation of AKT and poorer survival in patients with pancreatic cancer [34]. Therefore, our findings provide clinical relevance to the inhibition of AKT by PFTS and suggest that Ras inhibition could be beneficial in inhibiting downstream effectors such as AKT.

Combining agents for the treatment of cancer is a promising area of investigation [35]. The possible favorable outcomes for drug combinations include 1) increasing the efficacy of the therapeutic effect, 2) avoiding toxicity by decreasing drug dosage while increasing or maintaining the same efficacy, and 3) minimizing the development of drug resistance. Because of these benefits, drug combinations are being widely used and are an excellent choice for the treatment of cancer [35]. On the basis of the critical role that Kras and STAT3 play in pancreatic cancer [16,36], these pathways are attractive targets for drug development. Interestingly, PFTS is a successful combination partner of the novel STAT3 inhibitor P-V [23], the two of them synergizing to inhibit the growth of pancreatic cancer cells. We therefore believe that PFTS is a promising candidate agent for the treatment of pancreatic cancer and may also serve as a chemosensitizer to improve the therapeutic efficacy of other anticancer drugs.

In conclusion, the novel compound PFTS is an effective anticancer agent in preclinical models of pancreatic cancer, acting primarily through the inhibition of Kras activation and its downstream effectors. Taken together, our results point out to the potential of PFTS, a novel Ras inhibitor, as a new agent against pancreatic cancer and merit further evaluation.

References

[1] Hidalgo M (2010). Pancreatic cancer. *N Engl J Med* **362**, 1605–1617.

[2] Siegel R, Naishadham D, and Jemal A (2012). Cancer statistics, 2012. *CA Cancer J Clin* **62**, 10–29.

[3] Ying JE, Zhu LM, and Liu BX (2012). Developments in metastatic pancreatic cancer: is gemcitabine still the standard? *World J Gastroenterol* **18**, 736–745.

[4] Hruban RH, van Mansfeld AD, Offerhaus GJ, van Weering DH, Allison DC, Goodman SN, Kensler TW, Bose KK, Cameron JL, and Bos JL (1993). K-*ras* oncogene activation in adenocarcinoma of the human pancreas. A study of 82 carcinomas using a combination of mutant-enriched polymerase chain reaction analysis and allele-specific oligonucleotide hybridization. *Am J Pathol* **143**, 545–554.

[5] Morris JP IV, Wang SC, and Hebrok M (2010). KRAS, Hedgehog, Wnt and the twisted developmental biology of pancreatic ductal adenocarcinoma. *Nat Rev Cancer* **10**, 683–695.

[6] Botta GP, Reginato MJ, Reichert M, Rustgi AK, and Lelkes PI (2012). Constitutive *K-Ras*^{G12D} activation of ERK2 specifically regulates 3D invasion of human pancreatic cancer cells via MMP-1. *Mol Cancer Res* **10**, 183–196.

[7] Collisson EA, Trejo CL, Silva JM, Gu S, Korkola JE, Heiser LM, Charles RP, Rabinovich BA, Hann B, Dankort D, et al. (2012). A central role for RAF→MEK→ERK signaling in the genesis of pancreatic ductal adenocarcinoma. *Cancer Discov* **2**, 685–693.

[8] Gysin S, Lee SH, Dean NM, and McMahon M (2005). Pharmacologic inhibition of RAF→MEK→ERK signaling elicits pancreatic cancer cell cycle arrest through induced expression of p27^{Kip1}. *Cancer Res* **65**, 4870–4880.

[9] Milella M, Kornblau SM, Estrov Z, Carter BZ, Lapillonne H, Harris D, Konopleva M, Zhao S, Estey E, and Andreeff M (2001). Therapeutic targeting of the MEK/MAPK signal transduction module in acute myeloid leukemia. *J Clin Invest* **108**, 851–859.

[10] Wilhelm S and Chien DS (2002). BAY 43-9006: preclinical data. *Curr Pharma Des* **8**, 2255–2257.

[11] Chang F, Lee JT, Navolanic PM, Steelman LS, Shelton JG, Blalock WL, Franklin RA, and McCubrey JA (2003). Involvement of PI3K/Akt pathway in cell cycle progression, apoptosis, and neoplastic transformation: a target for cancer chemotherapy. *Leukemia* **17**, 590–603.

[12] Luo HR, Hattori H, Hossain MA, Hester L, Huang Y, Lee-Kwon W, Donowitz M, Nagata E, and Snyder SH (2003). Akt as a mediator of cell death. *Proc Natl Acad Sci USA* **100**, 11712–11717.

[13] Parsons CM, Muilenburg D, Bowles TL, Virudachalam S, and Bold RJ (2010). The role of Akt activation in the response to chemotherapy in pancreatic cancer. *Anticancer Res* **30**, 3279–3289.

[14] Bondar VM, Sweeney-Gotsch B, Andreeff M, Mills GB, and McConkey DJ (2002). Inhibition of the phosphatidylinositol 3′-kinase-AKT pathway induces apoptosis in pancreatic carcinoma cells *in vitro* and *in vivo*. *Mol Cancer Ther* **1**, 989–997.

[15] di Magliano MP and Logsdon CD (2013). Roles for KRAS in pancreatic tumor development and progression. *Gastroenterology* **144**, 1220–1229.

[16] Collins MA, Bednar F, Zhang Y, Brisset JC, Galban S, Galban CJ, Rakshit S, Flannagan KS, Adsay NV, and Pasca di Magliano M (2012). Oncogenic Kras is required for both the initiation and maintenance of pancreatic cancer in mice. *J Clin Invest* **122**, 639–653.

[17] Laheru D, Shah P, Rajeshkumar NV, McAllister F, Taylor G, Goldsweig H, Le DT, Donehower R, Jimeno A, Linden S, et al. (2012). Integrated preclinical and clinical development of S-*trans*, *trans*-farnesylthiosalicylic acid (FTS, Salirasib) in pancreatic cancer. *Invest New Drugs* **30**, 2391–2399.

[18] Rotblat B, Ehrlich M, Haklai R, and Kloog Y (2008). The Ras inhibitor farnesylthiosalicylic acid (Salirasib) disrupts the spatiotemporal localization of active Ras: a potential treatment for cancer. *Methods Enzymol* **439**, 467–489.

[19] Goldberg L, Haklai R, Bauer V, Heiss A, and Kloog Y (2009). New derivatives of farnesylthiosalicylic acid (Salirasib) for cancer treatment: farnesylthiosalicylamide inhibits tumor growth in nude mice models. *J Med Chem* **52**, 197–205.

[20] Huang L, Mackenzie G, Ouyang N, Sun Y, Xie G, Johnson F, Komninou D, and Rigas B (2011). The novel phospho-non-steroidal anti-inflammatory drugs, OXT-328, MDC-22 and MDC-917, inhibit adjuvant-induced arthritis in rats. *Br J Pharmacol* **162**, 1521–1533.

[21] Huang L, Mackenzie GG, Sun Y, Ouyang N, Xie G, Vrankova K, Komninou D, and Rigas B (2011). Chemotherapeutic properties of phospho-nonsteroidal anti-inflammatory drugs, a new class of anticancer compounds. *Cancer Res* **71**, 7617–7627.

[22] Mackenzie GG, Sun Y, Huang L, Xie G, Ouyang N, Gupta RC, Johnson F, Komninou D, Kopelovich L, and Rigas B (2010). Phospho-sulindac (OXT-328), a novel sulindac derivative, is safe and effective in colon cancer prevention in mice. *Gastroenterology* **139**, 1320–1332.

[23] Mackenzie GG, Huang L, Alston N, Ouyang N, Vrankova K, Mattheolabakis G, Constantinides PP, and Rigas B (2013). Targeting mitochondrial STAT3 with the novel phospho-valproic acid (MDC-1112) inhibits pancreatic cancer growth in mice. *PLoS One* **8**, e61532.

[24] Mackenzie GG, Queisser N, Wolfson ML, Fraga CG, Adamo AM, and Oteiza PI (2008). Curcumin induces cell-arrest and apoptosis in association with the inhibition of constitutively active NF-κB and STAT3 pathways in Hodgkin's lymphoma cells. *Int J Cancer* **123**, 56–65.

[25] Haklai R, Elad-Sfadia G, Egozi Y, and Kloog Y (2008). Orally administered FTS (salirasib) inhibits human pancreatic tumor growth in nude mice. *Cancer Chemother Pharmacol* **61**, 89–96.

[26] Mackenzie GG, Ouyang N, Xie G, Vrankova K, Huang L, Sun Y, Komninou D, Kopelovich L, and Rigas B (2011). Phospho-sulindac (OXT-328) combined with difluoromethylornithine prevents colon cancer in mice. *Cancer Prev Res (Phila)* **4**, 1052–1060.

[27] Lowenfels AB, Maisonneuve P, Cavallini G, Ammann RW, Lankisch PG, Andersen JR, Dimagno EP, Andrén-Sandberg A, and Domellöf L (1993). International Pancreatitis Study Group Pancreatitis and the risk of pancreatic cancer. *N Engl J Med* **328**, 1433–1437.

[28] Guerra C, Schuhmacher AJ, Cañamero M, Grippo PJ, Verdaguer L, Pérez-Gallego L, Dubus P, Sandgren EP, and Barbacid M (2007). Chronic pancreatitis is essential for induction of pancreatic ductal adenocarcinoma by K-Ras oncogenes in adult mice. *Cancer Cell* **11**, 291–302.

[29] Fukuda A, Wang SC, Morris JP IV, Folias AE, Liou A, Kim GE, Akira S, Boucher KM, Firpo MA, Mulvihill SJ, et al. (2011). Stat3 and MMP7 contribute to pancreatic ductal adenocarcinoma initiation and progression. *Cancer Cell* **19**, 441–455.

[30] Meyskens FL Jr, McLaren CE, Pelot D, Fujikawa-Brooks S, Carpenter PM, Hawk E, Kelloff G, Lawson MJ, Kidao J, McCracken J, et al. (2008). Difluoromethylornithine plus sulindac for the prevention of sporadic colorectal adenomas: a randomized placebo-controlled, double-blind trial. *Cancer Prev Res (Phila)* **1**, 32–38.

[31] Lesina M, Kurkowski MU, Ludes K, Rose-John S, Treiber M, Klöppel G, Yoshimura A, Reindl W, Sipos B, Akira S, et al. (2011). Stat3/Socs3 activation by IL-6 transsignaling promotes progression of pancreatic intraepithelial neoplasia and development of pancreatic cancer. *Cancer Cell* **19**, 456–469.

[32] Sun Y, Huang L, Mackenzie GG, and Rigas B (2011). Oxidative stress mediates through apoptosis the anticancer effect of phospho-nonsteroidal anti-inflammatory drugs: implications for the role of oxidative stress in the action of anticancer agents. *J Pharmacol Exp Ther* **338**, 775–783.

[33] Sun Y, Rowehl LM, Huang L, Machenzie GG, Vrankova K, Komninou D, and Rigas B (2012). Phospho-ibuprofen (MDC-917) suppresses breast cancer growth: an effect controlled by the thioredoxin system. *Breast Cancer Res* **14**, R20.

[34] Mortenson MM, Galante JM, Schlieman MG, and Bold RJ (2004). AKT: a novel target in pancreatic cancer therapy. *Cancer Ther* **2**, 227–238.

[35] Chou TC (2006). Theoretical basis, experimental design, and computerized simulation of synergism and antagonism in drug combination studies. *Pharmacol Rev* **58**, 621–681.

[36] Corcoran RB, Contino G, Deshpande V, Tzatsos A, Conrad C, Benes CH, Levy DE, Settleman J, Engelman JA, and Bardeesy N (2011). *STAT3* plays a critical role in *KRAS*-induced pancreatic tumorigenesis. *Cancer Res* **71**, 5020–5029.